Long period comet encounters with the planets: an analytical approach

G. B. Valsecchi
IAPS-INAF, Roma, Italy
IFAC-CNR, Sesto Fiorentino, Italy

The engine of cometary orbital evolution

- The orbital evolution of comets in the planetary region is mostly due to close encounters with the giant planets.
- An important parameter is the planetocentric velocity:
  - fast encounters – with hyperbolic planetocentric orbits – are effective only if deep;
  - slow encounters – with temporary satellite captures – can greatly modify cometary orbits even if rather shallow.
- Long-period comets practically never undergo "really slow" encounters.
- The outcomes can be extremely sensitive to initial conditions.

Sensitivity to initial conditions

LeVerrier was the first to show quantitatively the sensitivity to initial conditions in his study of the 1779 close encounter with Jupiter of comet Lexell.

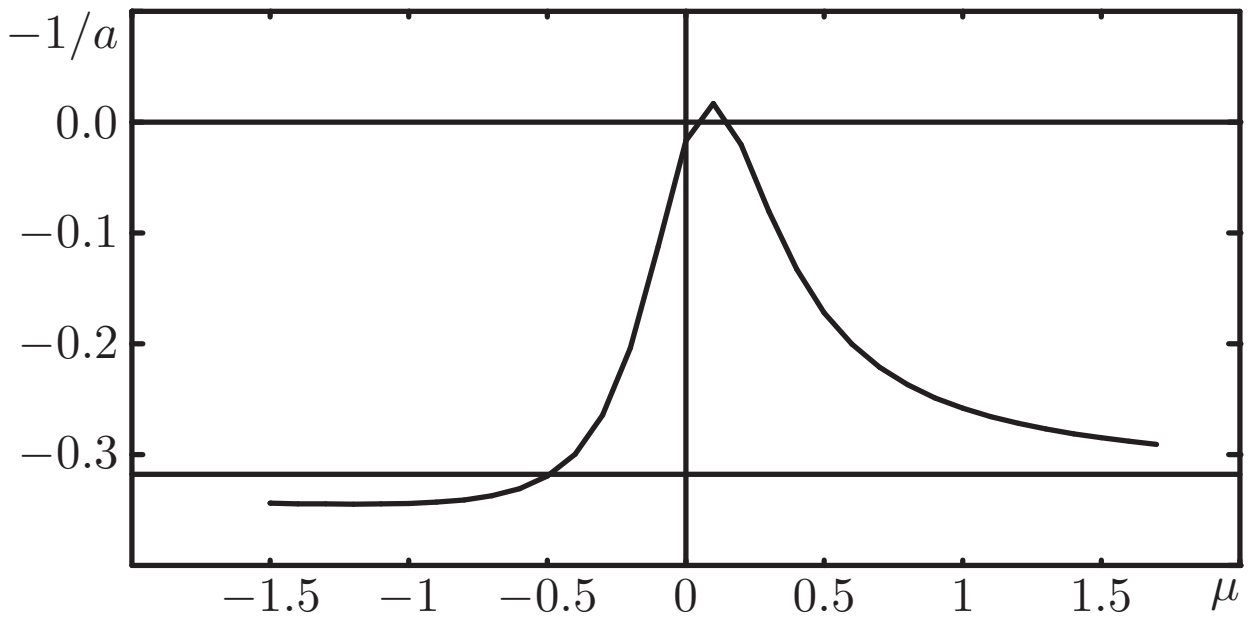

The post-1779 values of $-1/a$, in AU^{-1} given by LeVerrier as a function of μ; the lower horizontal line corresponds to the pre-1779 value of $-1/a$.

Why an analytical theory

The orbits of long period comets are not restricted to low inclinations; among the consequences of this, we have:

- wide range of encounter velocities;
- extended time spans without encounters, due to large Minimum Orbital Interception Distances (MOIDs) with the giant planets' orbits.

An analytical theory of close encounters can help to:

- identify regions of interest in the space of initial conditions, minimizing the need to run long numerical integrations in which "nothing happens";
- get a global understanding of the possible outcomes of close encounters.

Extended Öpik's theory of close encounters

Model: restricted, circular, 3-dimensional 3-body problem; far from the planet, the small body moves on an unperturbed heliocentric keplerian orbit.

The encounter with the planet: modelled as an instantaneous transition from the incoming asymptote of the planetocentric hyperbola to the outgoing one, taking place when the small body crosses the b-plane (O76, CVG90).

Our contribution: added equations to take into account the finite nodal distance and the time of passage at the relevant node (VMGC03, V06, VAR15).

Limitation: this model does not take into account the secular variation of the nodal distance, that has to be given as an additional input.

Encounter algorithm

pre-encounter		post-encounter
$a, e, i, \Omega, \omega, f_b$		$a', e', i', \Omega', \omega', f_b'$
$\downarrow$		$\uparrow$
X, Y, Z, U_x, U_y, U_z		$X', Y', Z', U_x', U_y', U_z'$
$\downarrow$		$\uparrow$
$U, \theta, \phi, \xi, \zeta, t_b$	$\Longrightarrow$	$U, \theta', \phi', \xi', \zeta', t_b$

The algorithmic path describing an encounter:

- we go from orbital elements to planetocentric coordinates and velocities describing a rectilinear motion;
- we pass from coordinates and velocities to Öpik variables;
- we apply the velocity vector rotation due to the encounter;
- we then retrace the same steps in the opposite order, back to orbital elements.

Geometric setup

The reference frame (X, Y, Z) is planetocentric, the Y-axis is in the direction of planet motion, the Sun is on the negative X-axis.

The direction of the incoming asymptote is defined by two angles, θ and ϕ, so that the planetocentric unperturbed velocity $\vec{U}$, in units of the heliocentric velocity of the planet, has components:

$$U_x = U \sin\theta \sin\phi; \quad U_y = U \cos\theta; \quad U_z = U \sin\theta \cos\phi.$$

As a consequence of an encounter the direction of $\vec{U}$ changes but its modulus U does not.

$$\begin{aligned} U &= U(a, e, i) \\ \theta &= \theta(a, e, i) = \theta(a, U) \\ \phi &= \phi(a, e, i, \mathrm{sgn}(\sin(f_b)), \\ &\quad \mathrm{sgn}(\cos(\omega + f_b))) \end{aligned}$$

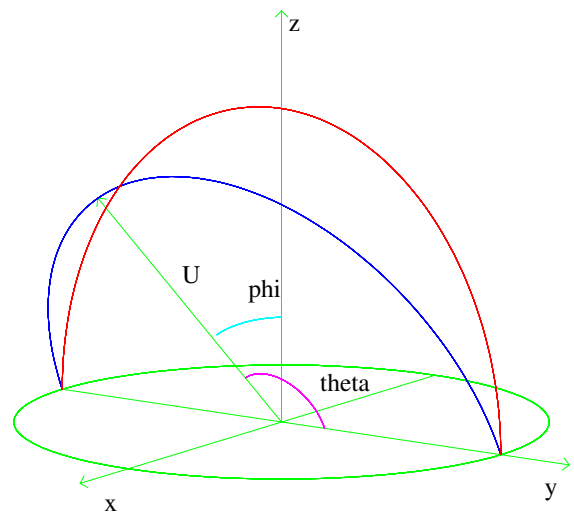

The b-plane

- The b-plane of an encounter is the plane containing the planet and perpendicular to the planetocentric unperturbed velocity $\vec{U}$.
- The vector from the planet to the point in which $\vec{U}$ crosses the plane is $\vec{b}$, and the coordinates of the crossing point are ξ, ζ.
- The coordinate $\xi = \xi(a, e, i, \omega, f_b)$ is the local MOID.
- The coordinate $\zeta = \zeta(a, e, i, \Omega, \omega, f_b, \lambda_p)$ is related to the timing of the encounter.

The b-plane circles

It is possible to show that the locus of b-plane points for which the post-encounter orbit has a given value of a', i.e. of θ', say a'_0 and θ'_0, is a circle (VMGC00) centred on the ζ-axis, at $\zeta = D$, of radius $|R|$, with

$$\begin{aligned} D &= \frac{c \sin\theta}{\cos\theta'_0 - \cos\theta} \\ R &= \frac{c \sin\theta'_0}{\cos\theta'_0 - \cos\theta}, \end{aligned}$$

where the scale factor $c = m/U^2$ is the value of the impact parameter corresponding to a velocity deflection of 90°.

The b-plane circles

Such a simple property reminds us of Galileo's words: "...[l'universo] è scritto in lingua matematica, e i caratteri son triangoli, cerchi, ed altre figure geometriche..."; it has interesting consequences:

- it is a building block of the algorithm allowing to understand the geometry of impact keyholes (VMGC03);
- it can be used to explain the asymmetric tails of energy perturbation distributions (VMGC00).

In the rest of the talk we discuss some properties of close encounters that can be deduced from this theory.

The b-plane circles

In practical applications, one has to keep in mind that:

- to each point on the b-plane of a close encounter corresponds one (and only one!) post-encounter orbit;
- for a given impact parameter b, the size of the resulting velocity deflection, and thus of the perturbation, depends on the ratio c/b, where b is the modulus of $\vec{b}$, and c is the scale factor already seen;
- a large velocity deflection does not necessarily imply a large semimajor axis perturbation.

Keyholes

A keyhole (Chodas 1999) is a small region of the b-plane of a specific close encounter of an asteroid with the Earth such that, if the asteroid passes through this region, it will hit the planet or have a very close encounter with it at a subsequent return.

The positions of keyholes in the b-plane of the encounter of 7 August 2027 of 1999 AN_{10}, for impacts in 2034, 2044, and 2046 (from Chodas 1999).

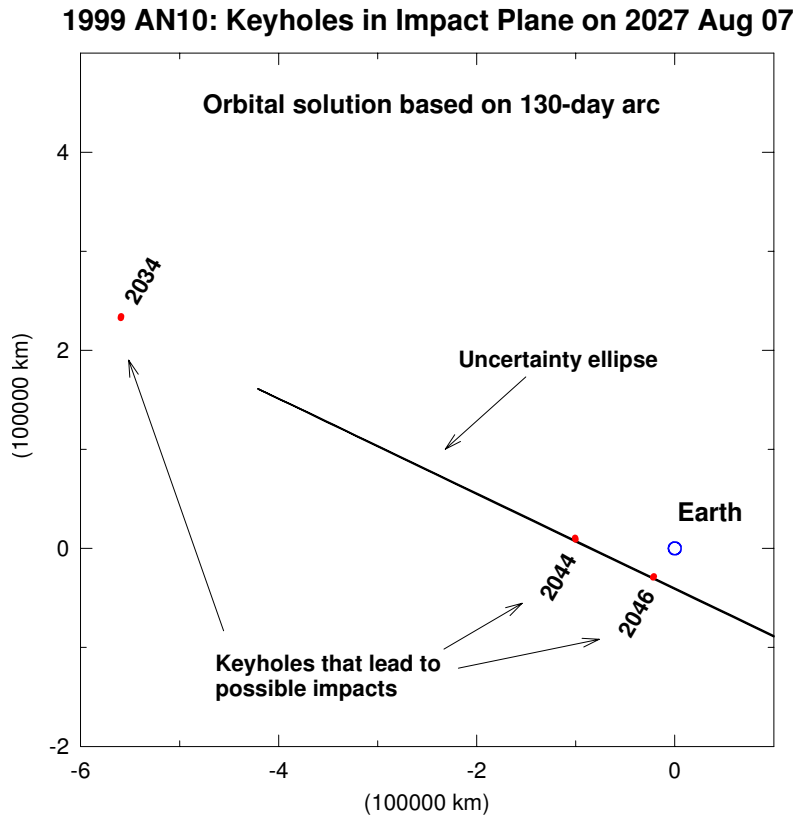

Keyhole locations

The positions of keyholes in the b-plane of the encounter of 7 August 2027 of 1999 AN_{10}, for a very close encounter in 2040 (from Chodas 1999).

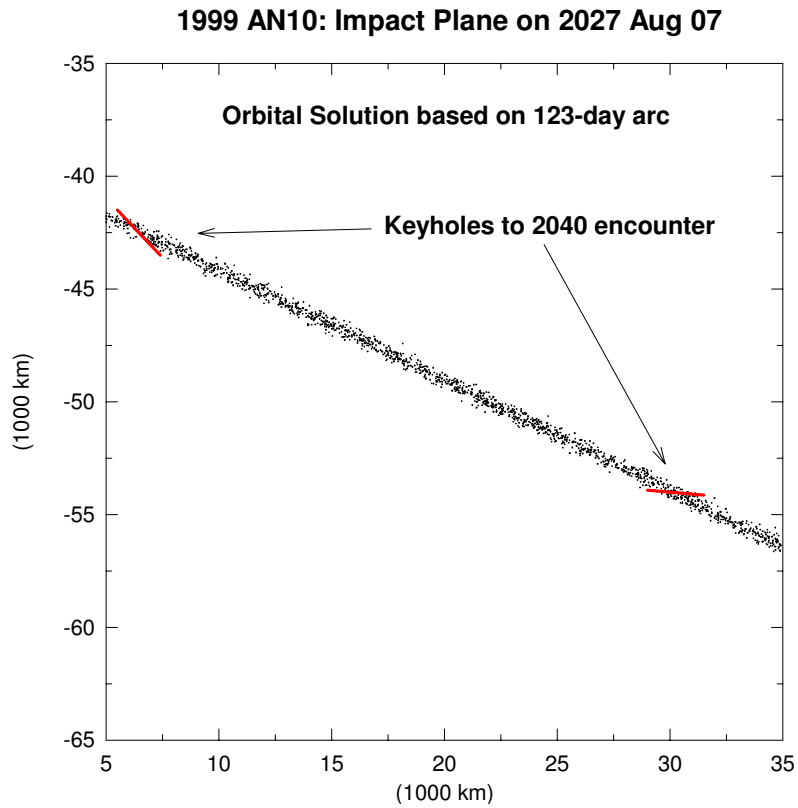

How good is the theory?

Keyholes are located at, or near to, the intersections of the Line of Variations (LoV) and the relevant b-plane circle.

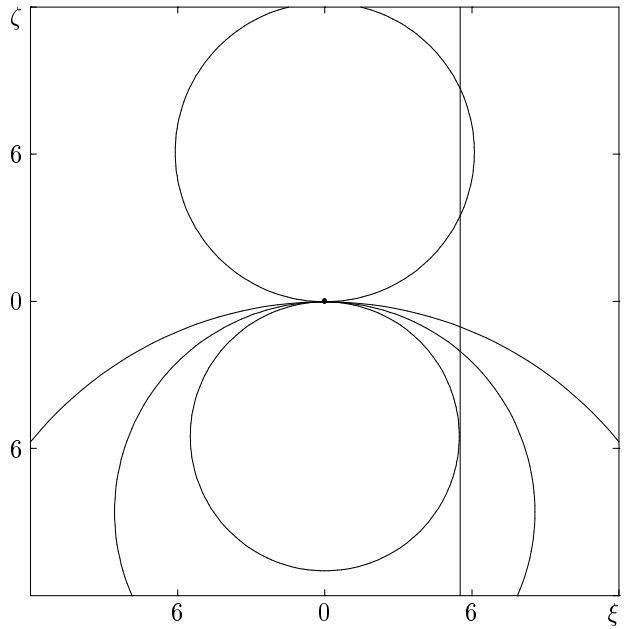

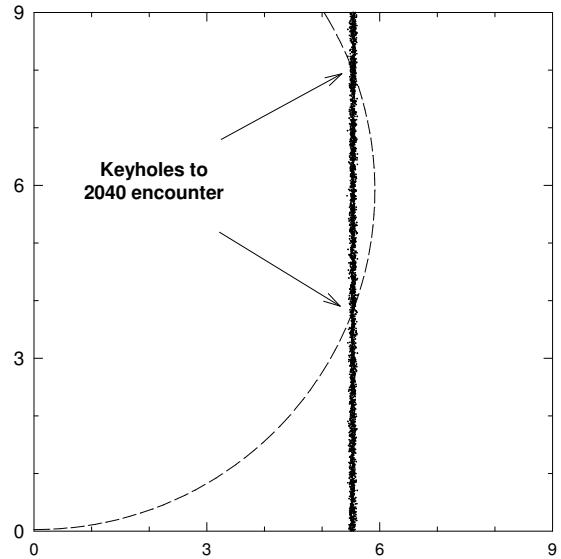

Left: b-plane circles for resonant return in 2040, 2030, 2044, 2046.
Right: Chodas' plot for 2040, suitably rotated; the circle comes from a best fit.

Shape and size of an impact keyhole

Problem: how varies the distance between two points of the b-plane of the current encounter when considering their images after propagation to the b-plane of the next encounter?

Result: the horizontal distance on the b-plane is essentially unchanged, the vertical one is stretched by a large factor, depending on the circumstances of the encounter.

Geometric consequence: the pre-image of the Earth on the b-plane of the encounter preceding the collision is a thick arclet closely following the shape of the circle corresponding to the suitable orbital period.

Apophis keyholes: theory

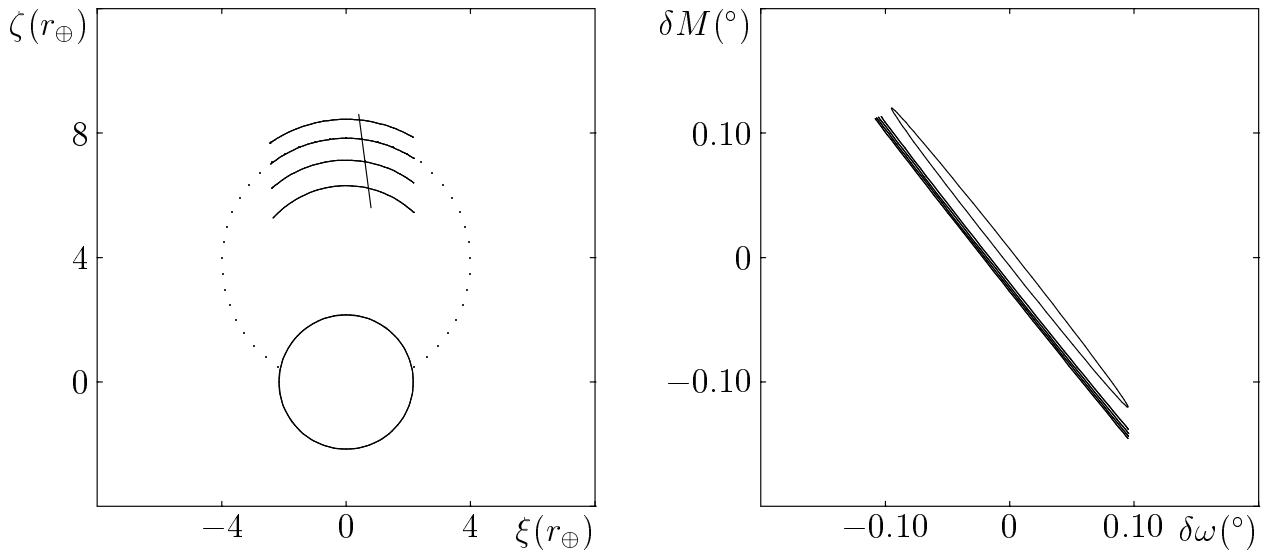

Left: LoV and theoretical keyholes for impacts in 2034, 2035, 2036, 2037 on the 2029 b-plane; Earth radius includes focussing, dots show the 6/7 resonance. Right: same keyholes, and pre-image of the Earth, in the $\delta\omega$-δM plane; the origin is a "central" 2029 collision.

Apophis 2036 keyhole: practice

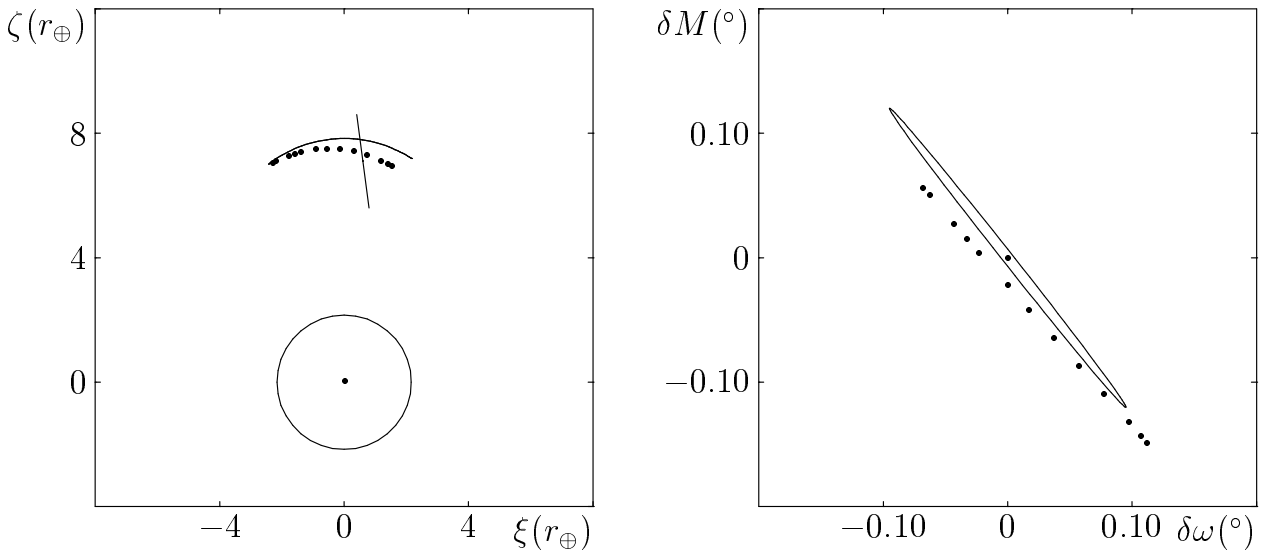

Left: LOV and 2036 theoretical keyhole, together with dots showing numerically found impact solutions; one of them is a "central" collision, the others are inside the "real" 2036 keyhole. Right: same impact solutions in the $\delta\omega$-δM plane.

Keyholes are useful

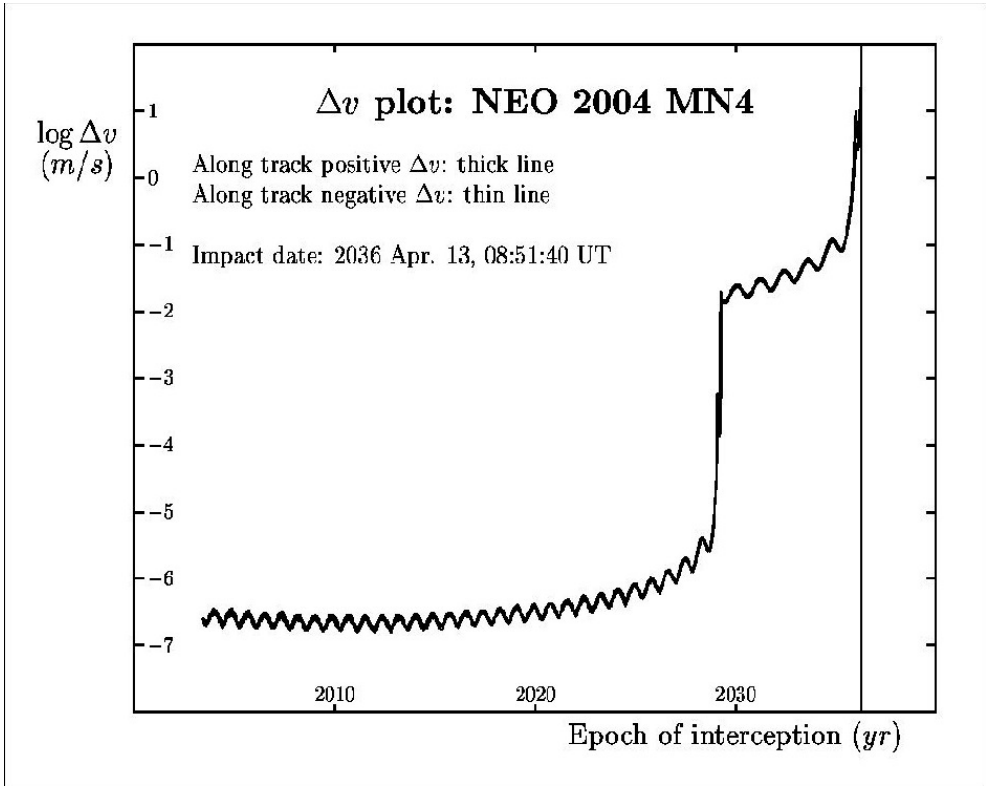

The ΔV necessary to avoid the 2036 collision of 2004 MN_4 with the Earth (Carusi 2005); the 2029 encounter lowers ΔV by four orders of magnitude.

The 2029 encounter of Apophis

On 13 April 2029 Apophis will encounter the Earth, and will be transferred into an Apollo orbit (it is currently an Aten).

We can visualize the b-plane circle within which Apophis has to pass in order to become an Apollo.

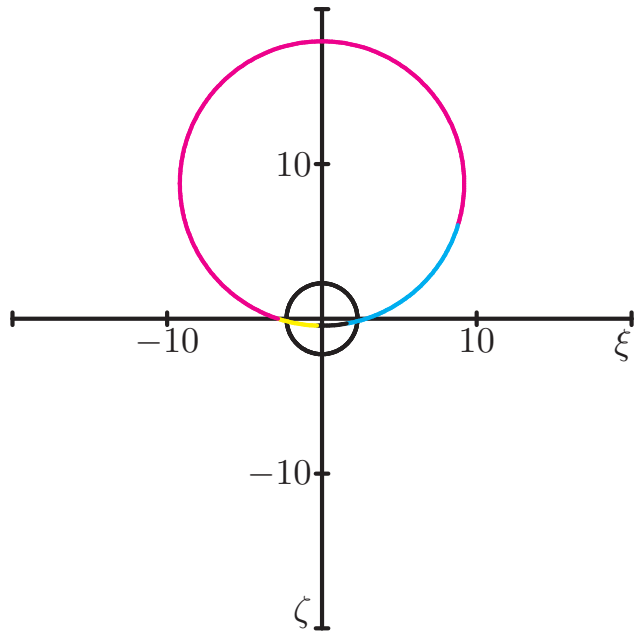

Colours give the post-encounter orbital geometry:

- magenta, ascending node, pre-perihelion;
- yellow, ascending node, post-perihelion;
- black, descending node, post-perihelion;
- cyan, descending node, pre-perihelion;

The distribution of energy perturbations

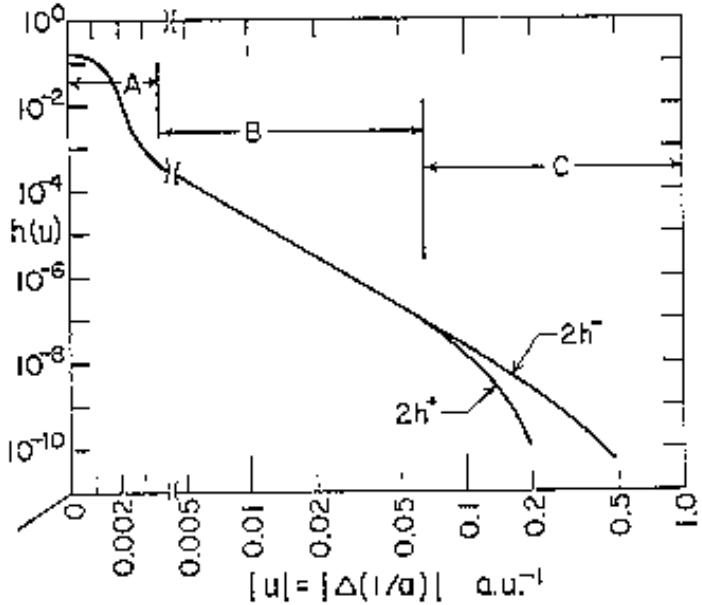

FIG. 1. The distribution $h(u)$ in energy changes u due to Jupiter is plotted vs $|u|$ for comets (otherwise random) whose Q value is 0.1 of Jupiter's orbital radius and whose inclination is 27°: The breaks in the lines indicate changeover from linear to logarithmic scales for $|u|$. The three regions A, B, and C are discussed in the text. The notation $2h^+$ indicates twice the distribution for the positive u values only, and $2h^-$ is the same for the negative u values.

The asymmetric energy perturbation distribution obtained numerically by Everhart (E69): the devil is in the (de)tails...

Cartography of the b-plane

Everhart's experiment: parabolic initial orbits, with $q/a_J = 0.1, i = 27^\circ$, i.e. $U = 1.48, \theta = 114^\circ$.

The plot shows some relevant b-plane circles.

Red circle: collisional cross section of Jupiter, of radius $b_c = 3.3 r_p$.

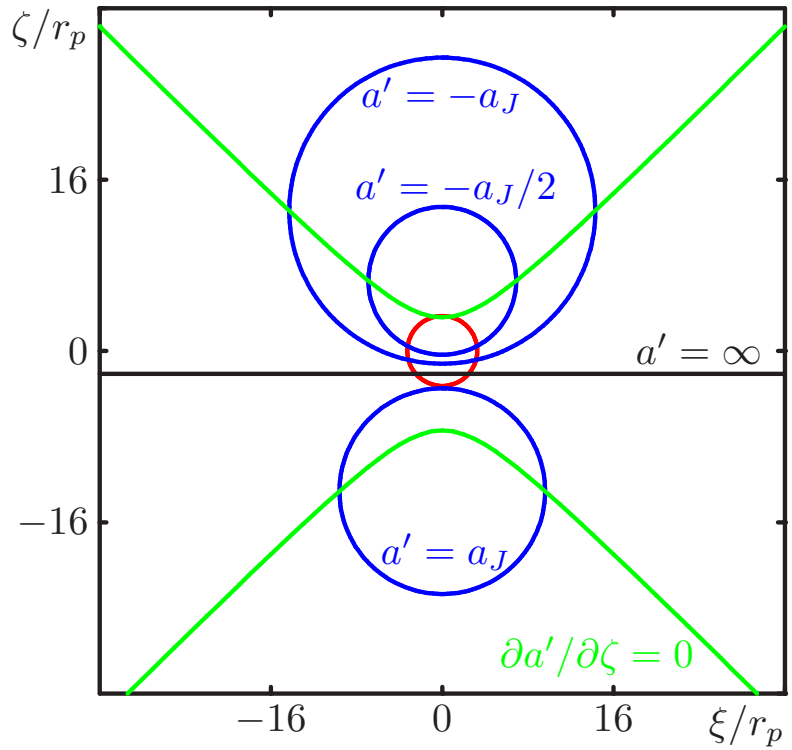

Horizontal line: parabolic post-encounter orbits.

Blue circles: post-encounter orbits with $a' = a_J, -a_J, -a_J/2$.

Green lines: conditions for $\partial a'/\partial\zeta = 0$.

Circles corresponding to different values of a' do not intersect.

Cartography of the b-plane

All of Everhart's orbits have the same probability of collision with Jupiter, since Öpik's collision probability per revolution depends on U, θ, ϕ (i.e., on a, e, i) and the cross-section of the planet:

$$\begin{aligned} P &= \frac{\sigma}{\pi \sin\theta |\sin\phi| \sin i} \\ &= \frac{b_c^2}{a_J^2} \frac{\sqrt{1 + 2U\cos\theta + U^2(1 - \sin^2\theta \sin^2\phi)}}{U \sin^2\theta |\sin\phi| |\cos\phi|}. \end{aligned}$$

If, instead of the planet cross-section, we consider the area of the circle corresponding to a certain post-encounter Δa, we obtain the probability of having a perturbation of size Δa or larger.

Cartography of the b-plane

Consider the circle for $a' = a_J$, within which one of Everhart's comets would be captured to an elliptical orbit of with $a' \leq a_J$.

Its area is 8.7 times larger than that the collisional cross-section of Jupiter.

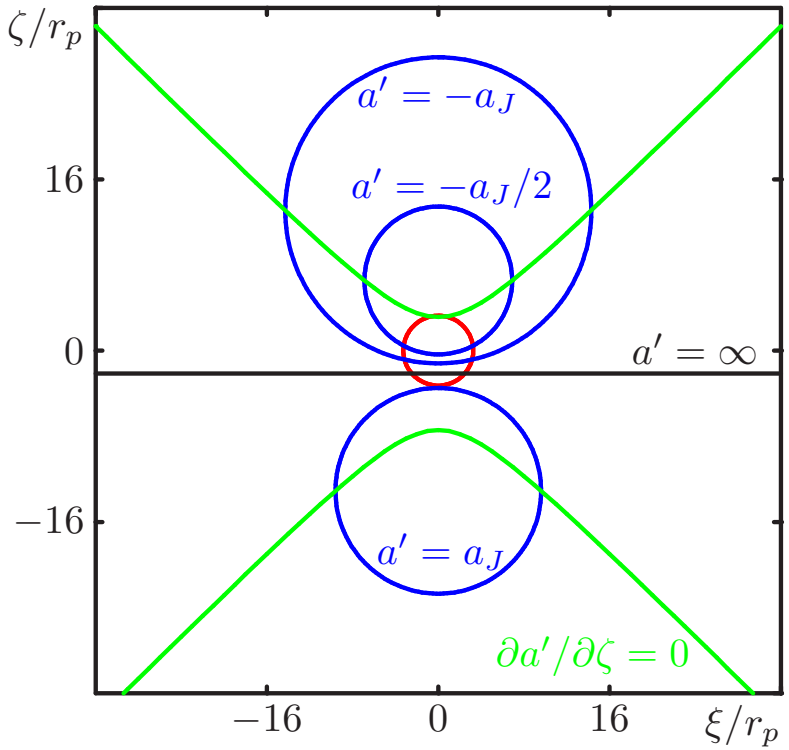

That is, for Everhart's experimental setup, capture to an orbit of period $P' \leq P_J$ is almost 9 times more frequent than collision with Jupiter.

The distribution of energy perturbations

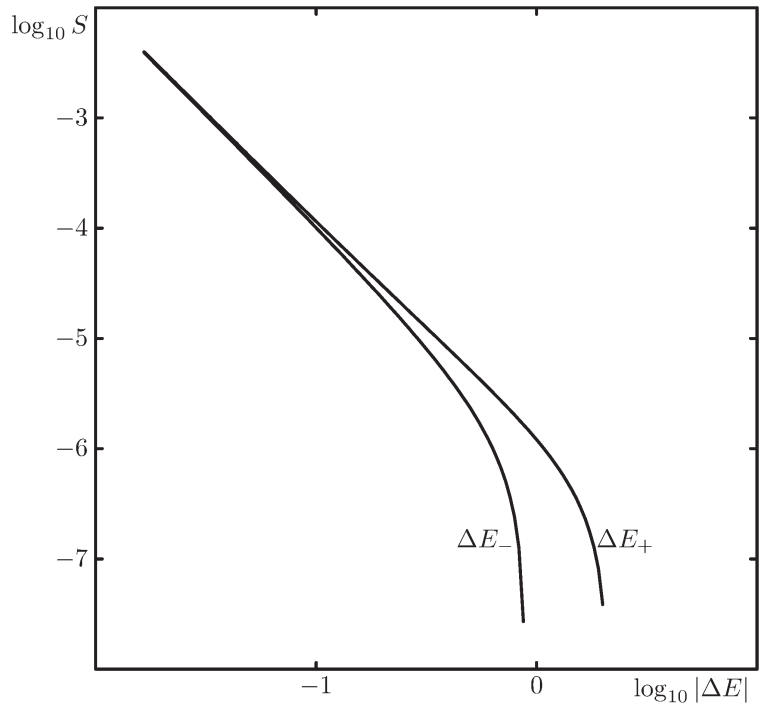

The analytical theory allows us to reproduce Everhart's asymmetric tails of the energy perturbation distribution.

Capture of parabolic comets to short-period orbits

Let us consider the efficiency of capture to orbits of $P \leq 200$ yr in the case of parabolic comets encountering one of the outer planets.

We consider three cases:

- very high planetocentric velocity, $U = 2$, i.e., twice the heliocentric velocity of the planet;
- high planetocentric velocity, $U = 1$, i.e., the same as the heliocentric velocity of the planet;
- moderately high planetocentric velocity, $U = 0.5$, i.e., half of the heliocentric velocity of the planet.

To each of these cases correspond suitable ranges of perihelion distances and inclinations.

Comet capture by Neptune

U	b_c	R	ρ	
2.0	2.4	2.6	1.2	red
1.0	4.5	19.2	18.6	blue
0.5	8.7	42.5	23.6	green

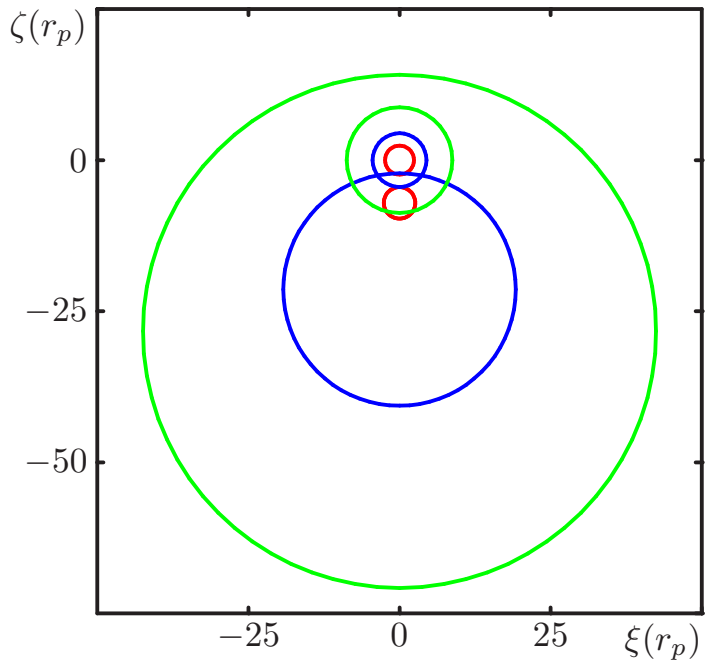

Capture to $P < 200$ yr of parabolic comets by Neptune.

The ratio $\rho = R^2/b_c^2$ is the ratio of capture and the collision cross sections.

For $U = 2$: $q = 30.1 \div 3.76$ au, $i = 110\overset{\circ}{.}7 \div 180^\circ$.

For $U = 1$: $q = 30.1 \div 15.1$ au, $i = 45\overset{\circ}{.}0 \div 0^\circ$.

For $U = 0.5$: $q = 30.1 \div 28.5$ au, $i = 13\overset{\circ}{.}5 \div 0^\circ$.

Comet capture by Jupiter

U	b_c	R	ρ	
2.0	2.5	43.0	293	red
1.0	4.7	139	872	blue
0.5	9.3	224	583	green

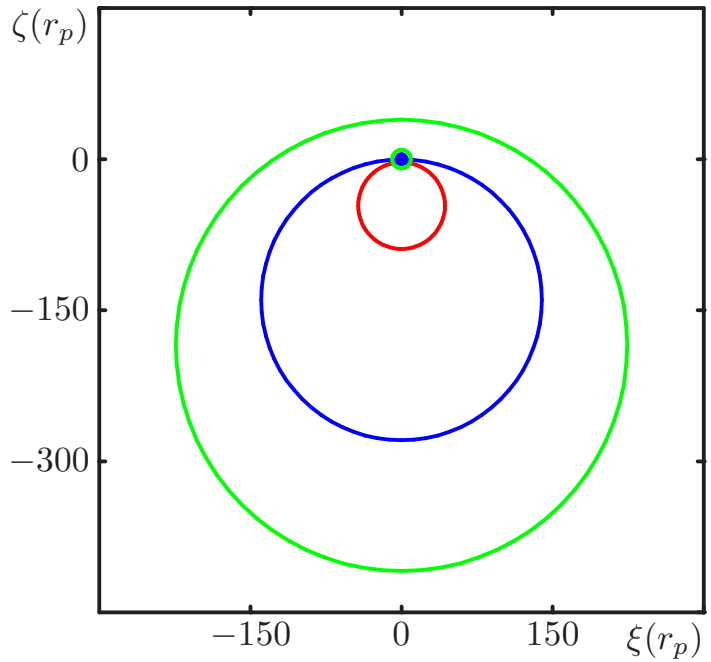

Capture to $P < 200$ yr of parabolic comets by Jupiter.

The ratio $\rho = R^2/b_c^2$ is the ratio of capture and the collision cross sections.

For $U = 2$: $q = 5.20 \div 0.65$ au, $i = 110\overset{\circ}{.}7 \div 180^\circ$.

For $U = 1$: $q = 5.20 \div 2.60$ au, $i = 45\overset{\circ}{.}0 \div 0^\circ$.

For $U = 0.5$: $q = 5.20 \div 4.92$ au, $i = 13\overset{\circ}{.}5 \div 0^\circ$.

Comet ejection by Jupiter

a	ρ	
a_J	0.26	red
$2a_J$	1.45	blue
$3a_J$	4.16	green

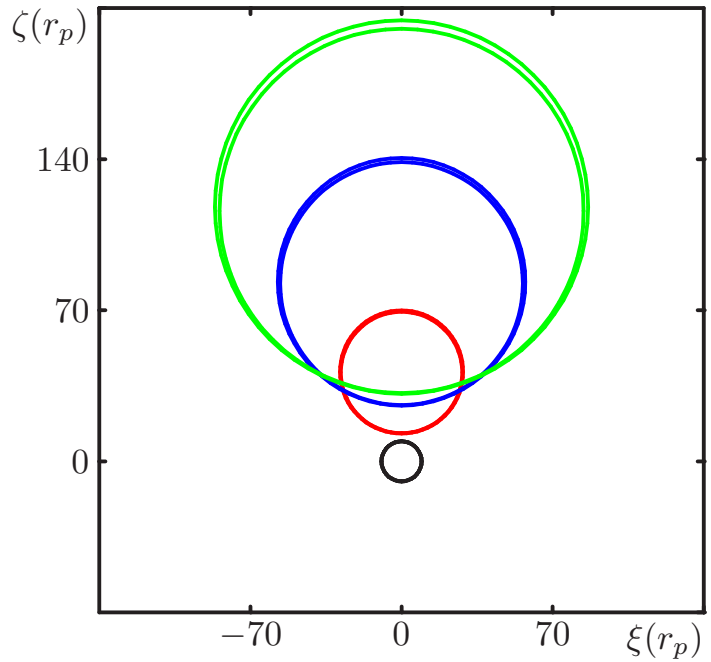

Efficiency of ejection to 1 000 au $< a' < \infty$ for comets encountering Jupiter with $U = 0.5$, relative to collision with the planet.

In this case, the cross sections ratio is $\rho = (R^2_{a'=1000} - R^2_{a'=\infty})/b_c^2$.

Comet ejection by Neptune

a	ρ	
a_N	1.39	red
$2a_N$	8.03	blue
$3a_N$	24.21	green

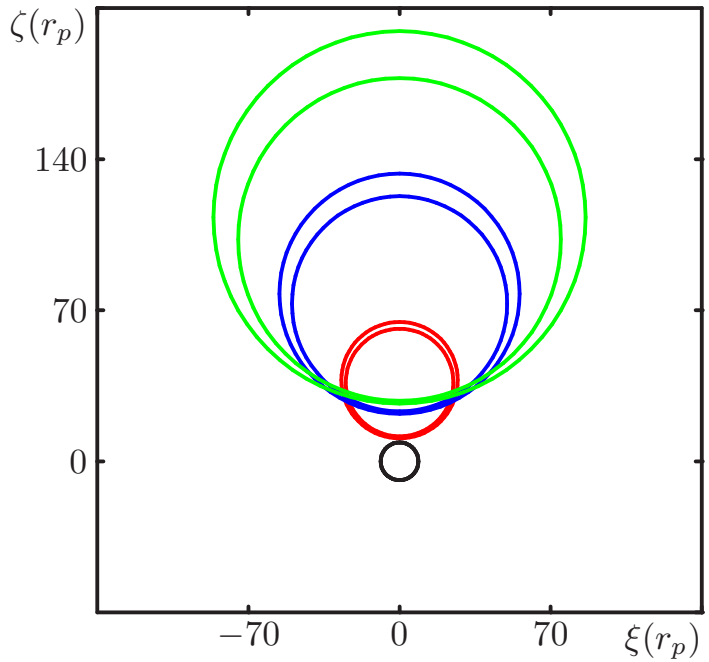

Efficiency of ejection to 1 000 au $< a' < \infty$ for comets encountering Neptune with $U = 0.5$, relative to collision with the planet.

In this case, the cross sections ratio is $\rho = (R^2_{a'=1000} - R^2_{a'=\infty})/b_c^2$.

Transition prograde→retrograde

Consider a prograde orbit of given a, e, i of a comet that can encounter Jupiter; is it possible that an encounter with the latter turns the orbit into a retrograde one?

And, if yes, under what conditions?

Let us start from the expressions of U and θ as functions of a, e, i:

$$\begin{aligned} U &= \sqrt{3 - \frac{a_p}{a} - 2\sqrt{\frac{a(1-e^2)}{a_p}}\cos i} \\ \cos\theta &= \frac{1 - U^2 - \frac{a_p}{a}}{2U}. \end{aligned}$$

Transition prograde→retrograde

For $i = 90°$, U becomes:

$$U = \sqrt{3 - \frac{a_p}{a}},$$

that implies:

$$\frac{a_p}{a} = 3 - U^2.$$

Substituting back in the expression for θ:

$$\cos\theta_{i=90°} = -\frac{1}{U}.$$

This implies that transitions to retrograde orbits can take place only if $U \geq 1$, no matter what the mass of the planet is.

Transition prograde→retrograde

Thus, to obtain a transition from prograde to retrograde, we need a close encounter that changes θ into $\theta' > \theta_{i=90^\circ}$.

This is something that we know how to obtain: the b-plane coordinates must be within the circle of radius $|R_{i'=90^\circ}|$ centred in:

$$\begin{aligned} \xi &= 0 \\ \zeta &= D_{i'=90^\circ}, \end{aligned}$$

with $D_{i'=90^\circ}, R_{i'=90^\circ}$ given by:

$$\begin{aligned} D_{i'=90^\circ} &= \frac{c \sin\theta}{\cos\theta'_{i'=90^\circ} - \cos\theta} \\ R_{i'=90^\circ} &= \frac{c \sin\theta'_{i'=90^\circ}}{\cos\theta'_{i'=90^\circ} - \cos\theta}. \end{aligned}$$

Transition prograde→retrograde

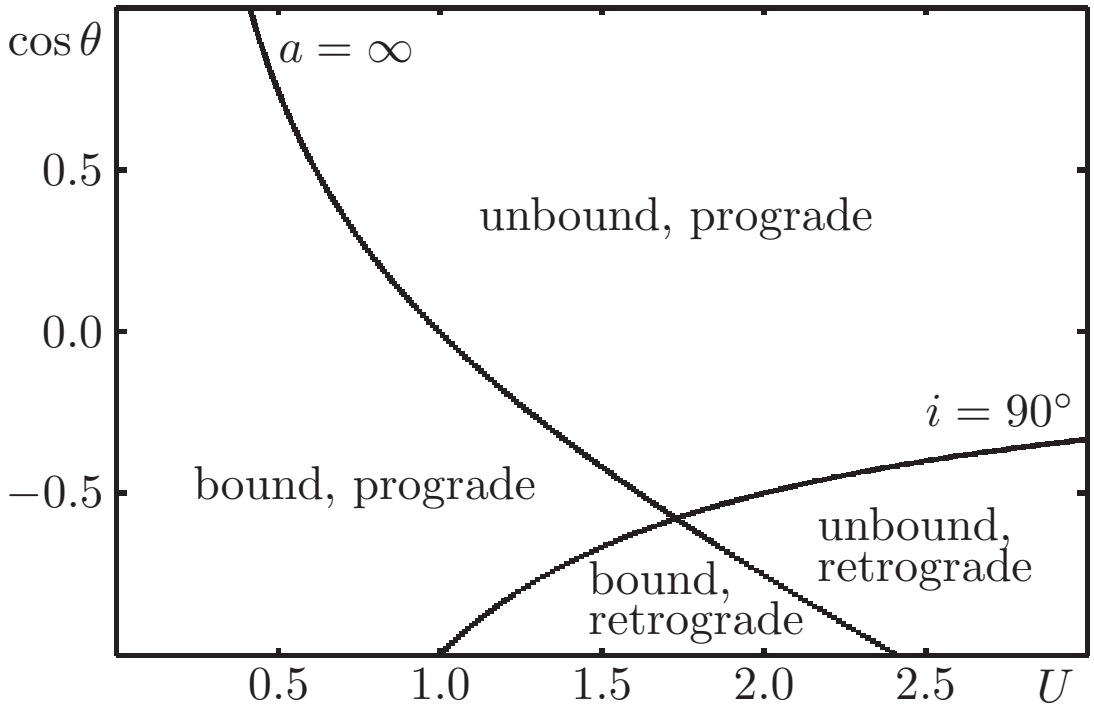

The plane U-$\cos\theta$; to each triple a, e, i corresponds a point in this plane.

Close encounters displace the orbit vertically in this plane.

Transition prograde→retrograde

For Everhart's parabolic comets ($q/a_J = 0.1$, $i = 27°$), the condition $i' = 90°$ implies:

$$a'_{i'=90°}/a_J = 1.26.$$

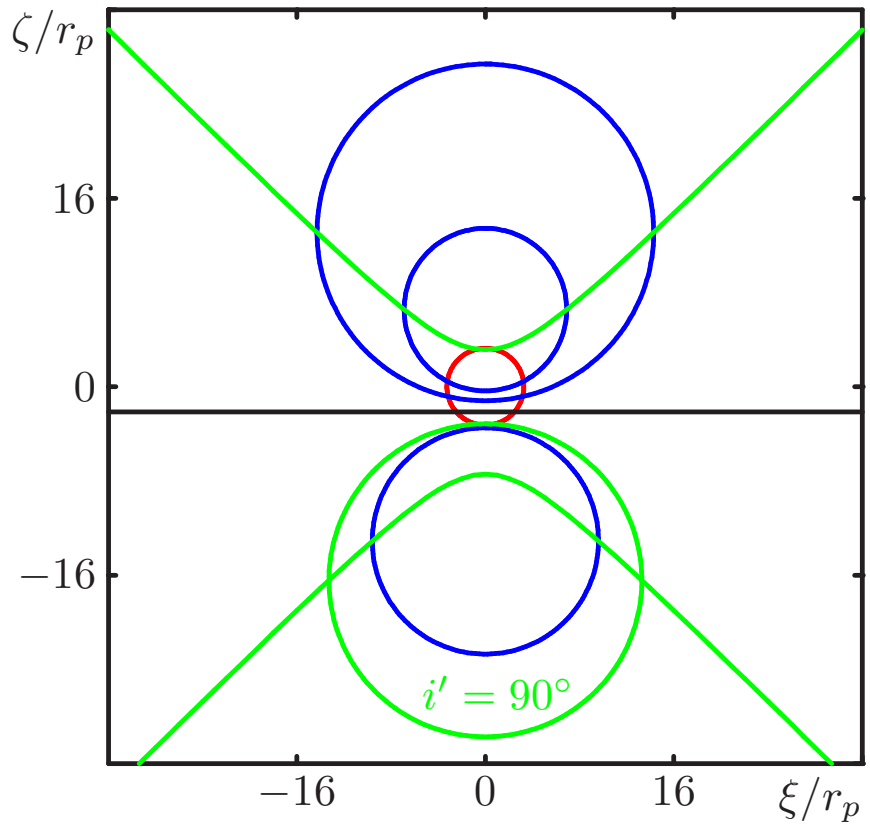

That is, all of Everhart's parabolic comets deflected in orbits of period $P \leq 1.41 P_J$ would be on retrograde post-encounter orbits.

Conclusions

The main merit of the analytical theory of close encounters is the geometric insight it provides into the problem; examples:

- the theory of resonant returns and keyholes;
- the explanation of the asymmetry of the tails of the energy perturbation distributions;
- the conditions leading to prograde-retrograde transitions and vice-versa.

Besides, its quantitative predictions can be useful in order to have a quick evaluation of the efficiency in some problems of orbital evolution dominated by planetary encounters.

References

- CVG90: Carusi A., Valsecchi G. B., Greenberg R., 1990, CeMDA 49,111
- E69: Everhart E., 1969, AJ 74, 735
- O76: Öpik E. J., 1976, Interplanetary Encounters, Elsevier
- V06: Valsecchi G. B., 2006, Lect. Notes Phys. 682, 145
- VMGC00: Valsecchi G. B., Milani A., Gronchi G. F., Chesley S. R., 2000, CeMDA 78, 83
- VMGC03: Valsecchi G. B., Milani A., Gronchi G. F., Chesley S. R., 2003, A&A 408, 1179
- VAR15: Valsecchi G. B., Alessi E. M., Rossi A., 2015, CeMDA 123, 151 (see also the Erratum, CeMDA 123, 167)